

Two Body Relaxation in Simulated Cosmological Haloes

Amr A. El-Zant

CITA, University of Toronto. Ontario M5S 3H8, Canada

12 June 2021

ABSTRACT

This paper aims at quantifying discreteness effects, born of finite particle number, on the dynamics of dark matter haloes forming in the context of cosmological simulations. By generalising the standard calculation of two body relaxation to the case when the size and mass distribution are variable, and parametrising the time evolution using established empirical relations, we find that the dynamics of a million particle halo is noise-dominated within the inner percent of the final virial radius. Far larger particle numbers ($\sim 10^8$) are required for the RMS perturbations to the velocity to drop to the 10% level there. The radial scaling of the relaxation time is simple and strong: $t_{\text{relax}} \sim r^2$, implying that numbers $\gg 10^8$ are required to faithfully model the very inner regions; artificial relaxation may thus constitute an important factor, contributing to the contradictory claims concerning the persistence of a power law density cusp to the very centre. The cores of substructure haloes can be many relaxation times old. Since relaxation first causes their expansion before recontraction occurs, it may render them either more difficult or easier to disrupt, depending on their orbital parameters. It may thus modify the characteristics of the subhalo distribution; and, if as suggested by several authors, it is parent-satellite interactions that determine halo profiles, the overall structure of the system may be affected. We derive simple closed form formulas for the characteristic relaxation time of both parents and satellites, and an elementary argument deducing the weak N -scaling reported by Diemand et al. (2004) when the main contribution comes from relaxing subhaloes.

Key words: dark matter – galaxies: haloes – diffusion – galaxies: general – galaxies: formation – galaxies: structure

1 INTRODUCTION

N -body modelling of the dynamical evolution of the dark matter component involves the approximation whereby the system to be simulated is represented by a surrogate one consisting of many order of magnitudes fewer particles. Discreteness noise is thus necessarily greatly enhanced. Furthermore, within the context of the cold dark matter scenario, material rapidly collapses into haloes; in a hierarchical process that ensures that the first structures are badly resolved, with particle noise propagating through the hierarchy, further enhancing discreteness effects and weakening the N -dependence of the effective relaxation time (Binney & Knebe 2002; Diemand et al. 2004).

Relaxation is expected to play its most prominent role in the very central regions of collapsed structures — precisely the place where there remains considerable controversy as to whether the slope of the density profile persists as a power law up to the resolution limit (Diemand et al. 2005), or instead gradually flattens into a smooth core (Navarro

et al. 2004). From the difference between these two situations follow important implications concerning the compatibility of the cold dark matter scenario with the observed inner mass distribution in galaxies. Relaxation also affects the symmetry of a system in physical and velocity space, rendering it more isotropic; and triaxial haloes may play an important role in determining the dynamics of the baryonic component (e.g., El-Zant & Shlosman 2002; El-Zant et al. 2003).

Since substructure haloes are resolved with far fewer particles, relaxation is expected to have a more dominant effect on their internal structure and (by modifying the efficiency of stripping) their spatial distribution. If accretion and merging are dominant processes in determining them (Syer & White 1998; Dekel et al. 2003b; Dekel et al. 2003a), this will have important implications for the parent halo properties too.

Estimating the importance of particle noise in N -body simulations is an essential step in evaluating the role it may

arXiv:astro-ph/0506617v1 25 Jun 2005

play in determining the dynamical state of collapsed structures. Our focus here is on the generalisation of the standard formulation of the problem, leading to the familiar formulas for the ‘relaxation time’ in stellar systems, to the cosmologically relevant case, when the physical extent and the mass distribution of the object under consideration continuously vary with time. The details of the procedure, along with the assumptions involved, are outlined in Section 2. In our treatment we will distinguish between ‘parent’ haloes, representing the most massive progenitors and ‘subhaloes’, representing the substructure. The former are assumed to continue to grow in mass and size, while the latter’s growth stops once they are incorporated into a larger structure. In both cases we derive simple formulas for calculating characteristic relaxation times (Section 3) and, in addition, undertake a more detailed calculation of the expected *root mean square (RMS)* perturbation to trajectories’ velocities for haloes evolving in the context of the ‘concordance’ CDM model; giving simple empirical fits to the results (Section 4). Conclusions are summarised in Section 5.

2 THE MODEL

We are interested in the description of relaxation due to discreteness (particle) noise in evolving cosmological haloes. The model through which this is done is described below. First the time evolution of the halo mass distribution is parametrised; the standard description of relaxation in gravitational systems is then generalised to encompass the case of these evolving systems.

2.1 Evolution of the halo mass distribution

Describing the temporal evolution of the halo mass distribution is simplified by the fact that their densities can always be approximately parametrized by double power law functions, independently of the mass of the halo, or the redshift at which it is identified. Two profiles have been extensively used: that introduced by Navarro, Frenk & White 1997 (NFW) has density $\sim 1/r$ in the inner region and $\sim 1/r^3$ in the outer one; the associated mass fraction within radius r is

$$\frac{M(r)}{M(r_{\text{vir}})} = \frac{\ln(1+r/r_s) - \frac{r/r_s}{1+r/r_s}}{\ln(1+c) - \frac{c}{1+c}}. \quad (1)$$

The profile put forward by Moore et al. 1999 (M99) has similar asymptotic density variation at large r , but a steeper central cusp ($\sim 1/r^{3/2}$). It has mass distribution

$$\frac{M(r)}{M(r_{\text{vir}})} = \frac{\ln[1+(r/r_s)^{3/2}]}{\ln(1+c^{3/2})}. \quad (2)$$

In these formulas, r_s is the characteristic halo scale length (separating the $1/r$ from the $1/r^3$ region) and r_{vir} is the virial radius. Their ratio $c = r_{\text{vir}}/r_s$ determines the mean density contrast inside radius r : $\Delta = \frac{M(r)}{M(r_{\text{vir}})} \frac{r_{\text{vir}}^3}{r^3}$ (cf. Fig 1).

The virial radius is usually defined as the radius inside which the average density is ~ 200 times the critical density

for closure ρ_c . Relative to ρ_c , the mean density contrast inside r is

$$\nu = \frac{\rho(r)}{\rho_c} = 200 \times \Delta = 200 \frac{M(r)}{M(r_{\text{vir}})} \frac{r_{\text{vir}}^3}{r^3}. \quad (3)$$

In a universe with matter and vacuum energy densities such that $\Omega_m(z) + \Omega_V(z) = 1$, the virial radius varies with redshift as

$$\frac{r_{\text{vir}(z)}}{r_{\text{vir}(0)}} = \frac{(M(r_{\text{vir}}, z)/M_0)^{1/3}}{(\Omega_m(1+z)^3 + \Omega_V)^{1/3}}, \quad (4)$$

where $M_0 = M(r_{\text{vir}}, z = 0)$. Wechsler et al. (2002) suggested the empirical relation whereby

$$M_{\text{vir}}(z) = M_0 e^{-\alpha z}. \quad (5)$$

This defines a characteristic halo growth time¹

$$\tau_s \sim \left(\frac{d \ln M}{dt} \right)^{-1} = \frac{-1}{\alpha dz/dt}. \quad (6)$$

The parameter $\alpha \sim 1$ varies systematically with halo mass (but appears constrained to the range $0.4 \lesssim \alpha \lesssim 1.6$). In this paper we fix $\alpha = 1$, noting that our results were found to be quite insensitive as to the exact choice of α . Wechsler et al. also find that, for NFW type fits to the density profile, $c \sim (1+z)^{-1}$, with an average value of order 10 at $z = 0$. Their results thus generally confirmed the prescription (due to Bullock et al. 2001)

$$c[\text{NFW}, z] = \frac{9}{1+z}, \quad (7)$$

which is used here. We assign a minimal value of $c = 9/5$ at high z (because structures with $\rho \sim 1/r$ in their outer regions are necessarily far from virial equilibrium; the simulations of Bullock et al. 2001; Zhao et al. 2003 and Tasitsiomi et al. 2004 confirm the presence of a minimal c). The concentration parameter of an M99 fit relates to that of an NFW fit through $c[\text{M99}] \approx (c[\text{NFW}]/1.7)^{0.9}$.

For any given z there is a mass dependent spread in c ; it is given, in terms of the typical mass scale $M_*(z)$ collapsing at redshift z , via $c \sim (M_{\text{vir}}/M_*)^{-0.13}$. Nevertheless, this relation shows that, even for a halo that is ten orders of magnitude more massive than M_* , c only changes by a factor of ten. From Fig. 1, this leads to a corresponding change in the density contrast of about the same factor or less. But since the relaxation time (cf, Eq. 15 below) $\sim N(r)\tau_D(r) \sim \sqrt{\rho(r)}$ inside any fixed radius; it changes by a factor of only a few even for such a highly unlikely mass deviation. Trials with different normalisations in Eq. (7), and with the prescription proposed by (Eq. 10 of) Zhao et al. (2003), have confirmed this. In fact it turns out (Section 4.2) that the relaxation rate is quite a strong function of radius, and will be important at small radii for any reasonable set of c values during the evolution. The results presented in this paper assume the

¹ The exponential form reflects a two phased evolution; a period of rapid accretion followed by slower growth. Zhao et al. (2003) have confirmed its basic premises for halos growing through almost four orders of magnitudes in mass and three in radius (although they do not use this particular form to fit the data).

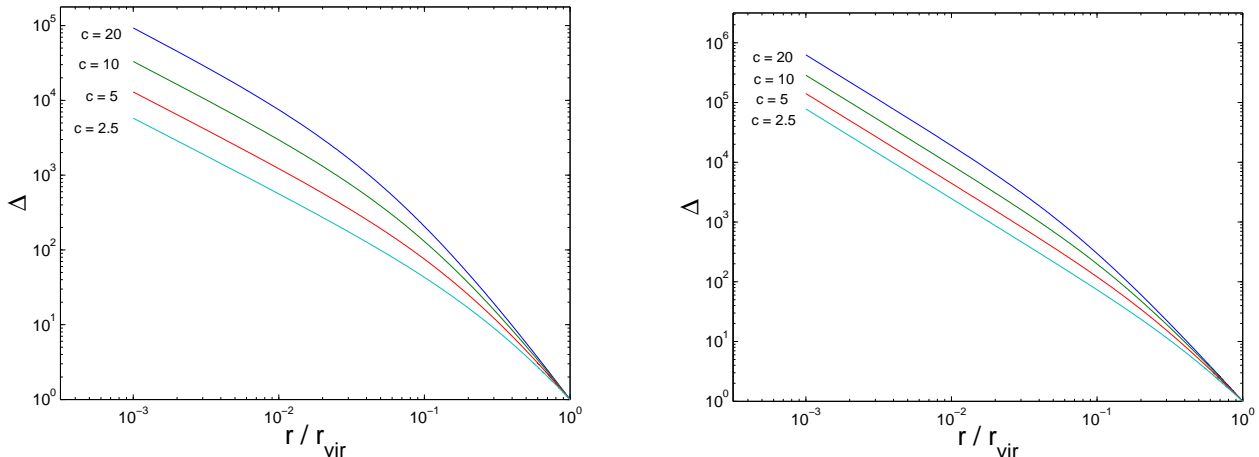


Figure 1. Density contrast Δ , measured relative to the average density within the virial radius, for NFW (left) and M99 profiles with different values for the concentration parameters c

quoted form for this relation, ignoring the weak mass dependence. Remarkably, our general conclusions should hold for haloes in any mass range

2.2 Generalisation of the standard formulation

The standard approach to relaxation in gravitational systems has developed along the foundation set by Chandrasekhar (1943). In analogy with the case of dilute gases, it is assumed that perturbations experienced by a test particle arise from independent and local two body encounters. Since the mean field along a particle's trajectory changes on a timescale comparable to its dynamical time τ_D , while the timescale of an average encounter is $\sim \tau_D/N$, this assumption is generally satisfied; encounters with duration $\sim \tau_D$ being relatively rare. As the number of particles in the representation of a self-gravitating system is increased, the effect of strong encounters becomes increasingly unimportant; in softened systems, the subject of cosmological simulations, strong encounters are completely suppressed if the softening length is of the order of the interparticle distance. The standard formulation of relaxation theory therefore assumes that the effect of discreteness noise can be modelled in the form of weak random encounters. Numerical tests (e.g., Huang, Dubinsky & Carlberg 1993), seem to vindicate these basic premises.²

The product of weak, local and independent encounters is a diffusion process, whereby a particle's dynamical variables undergo a random walk around their unperturbed values. For a spherical system with isotropic velocities that

can be approximated in terms of a Maxwellian, the mean diffusion coefficient within radius r

$$\langle (\Delta v)^2 \rangle = \frac{G^2 \rho m \ln \Lambda}{K \sigma} \quad (8)$$

describes the average *rate* at which the square velocities of particles deviate from those of unperturbed trajectories in a corresponding smooth system (with $N \rightarrow \infty$). Here Λ is the ratio of maximum to minimum impact parameters and $K = 1/15.4$ (according to Spitzer & Hart 1971). *In quasiequilibrium, at any given instant*, the average velocity dispersion inside radius r can be calculated from

$$\sigma^2(r) = \frac{3}{r} \int_0^r \bar{v}_r^2 dr = \gamma^2 v_c^2 = \gamma^2 GM/r = \gamma^2 G \frac{4}{3} \pi \rho r^2. \quad (9)$$

The local one dimensional velocity dispersion \bar{v}_r^2 can be evaluated by solving the Jeans equation (cf. Appendix B). The above relations thus define the weak function of radius γ that is used in the calculations below. This definition should hold because the virialised region of a cosmological halo remains near equilibrium through most of its evolution — major mergers being relatively rare, and even when they do occur the system is out of equilibrium for a time τ_D generally much smaller than the (relaxation) timescales of interest.

When the system parameters are changing, as during the growth of a cosmological halo, the mass inside any given radius will be time dependent. As a consequence, there will be corresponding variations in $\rho = \frac{M(r,t)}{4/3\pi r^3}$ and γ . Nevertheless, if the timescale between encounters giving rise to the relaxation process ($\tau_e \sim \tau_D/N$) is much smaller than the timescale for variation of the system parameters τ_s , then local (in time) averages are allowed, and the diffusion coefficient becomes a well defined function of time. From Eq. (6), and because

$$|\dot{z}| = (1+z) H \quad (10)$$

and

² Note nevertheless that such work generally focused on energy changes along particle trajectories. The response of the trajectories themselves (and thus the effect on quantities like angular momentum) can exhibit significantly stronger sensitivity to noise — even in the simplest case of deflections caused by fixed background particles (Athanasoula et al. 2001; El-Zant 2002).

$$\rho_c = \nu \frac{3H^2}{8\pi G}, \quad (11)$$

one finds that $t_s \sim \frac{1}{1+z} \sqrt{\frac{3}{8\pi G \rho_c}}$. Therefore, unless z is very large, $\tau_s > \tau_D \sim 1/\sqrt{\nu G \rho_c}$ (recall that $\nu \geq 200$); with the implication that the temporal locality condition ($\tau_e \ll \tau_s$) is in fact weaker than that for spatial locality ($\tau_e \ll \tau_D$), required for the validation of the diffusion approach.

The expression for the mean diffusion coefficient, inside radius r and at time t , can then be written as

$$\frac{\langle(\Delta v)^2\rangle(r, t)}{\sigma^2(r, t)} = \frac{\sqrt{G\rho(r, t)}}{K\gamma^3(r, t)\sqrt{4\pi/3}} \frac{m}{M(r, t)} \ln \Lambda(r, t). \quad (12)$$

The relative mean square perturbation to particle velocities due to encounters with other particles during the halo evolution is

$$\langle v_p^2/\sigma^2 \rangle = \int_{t_f}^{t_0} \frac{\langle(\Delta v)^2\rangle(r, t)}{\sigma^2(r, t)} dt, \quad (13)$$

where t_f refers to some chosen initial, reference, formation time (for any given r measured at $z = 0$, we will take the redshift to be the time when $r_{\text{vir}}(t_f) = r$) and t_0 refers to the end of the simulation (assumed to correspond to $z = 0$).

Using (12) and (13) one can define the relaxation time in a simulated cosmological halo implicitly:

$$\langle v_p^2/\sigma^2 \rangle(t_{\text{relax}}) = \int_{t_f}^{t_{\text{relax}}} \frac{\sqrt{G\rho}}{K\gamma^3\sqrt{4\pi/3}} \frac{m}{M} \ln \Lambda dt = 1. \quad (14)$$

If $t_{\text{relax}} \lesssim t_0$ the dynamics can be expected to be completely dominated by discreteness noise. This is in line with the standard application to time independent systems, where $t_f = 0$ and $\langle v_p^2/\sigma^2 \rangle$ is assumed to be time independent; the the result are the familiar expressions for the relation time

$$t_{\text{relax}} = K \frac{\sigma^3}{G^2 \rho m \ln \Lambda} = \frac{K\gamma^3 \sqrt{\frac{4}{3}\pi} M}{\ln \Lambda \sqrt{G\rho}} \frac{m}{m} \sim 0.1 \frac{N}{\ln \Lambda} \tau_D \quad (15)$$

(where $N(r)$ and $\tau_D(r)$ are the particle numbers and mean dynamical time inside r).

To fix the value of Λ , we assume that the resolution of the simulations in question corresponds to the local interparticle distance. The average of this quantity within radius r will define the minimum impact parameter $b_{\text{min}} = (\frac{4}{3}\pi r^3/N(r))^{1/3}$. The maximum impact parameter will be taken to correspond to the virial radius. We therefore have

$$\Lambda(r, t) = \frac{b_{\text{max}}}{b_{\text{min}}} = \left(\frac{3}{4\pi}\right)^{1/3} N^{1/3}(r, t) \frac{r_{\text{vir}}(t)}{r}. \quad (16)$$

3 SIMPLE ESTIMATES

In the next section we will numerically evaluate the integral in Eq. (14), invoking the time dependence appropriate in the currently favoured Λ CDM cosmology. Some insight can however be gained by defining characteristic relaxation times for an evolving cosmological halo and for its substructure. This is the subject of this section.

3.1 A characteristic relaxation time for cosmological haloes

We consider first the evolution of the parent halo, or most massive progenitor, and assume that all mass is added to it in the form of a smooth component. Of course, in reality, accretion of material takes the form of clumpy subhaloes, but most of their mass is rapidly stripped, so that, at any given time, there is usually only 10 – 20% of the mass of the halo in the substructure. Their internal relaxation is dealt with separately below.

If the relaxation time within some radius r is smaller than the timescale τ_s for the mass distribution to significantly evolve, it is likely that the system is heavily affected by discreteness noise within radius r — the rationale being that if the local relaxation time is small compared to the time it takes for more particles to be added to the system (thus decreasing the relaxation rate) then discreteness noise will have a significant effect.

A local relaxation time can be obtained by freezing the system at some time $t = t(z)$ and using (15). Comparing the two timescales one can write

$$R = t_{\text{relax}}/\tau_s = \frac{K\alpha\gamma^3 \sqrt{\frac{4}{3}\pi} |dz/dt| M}{\ln \Lambda \sqrt{G\rho} m}, \quad (17)$$

and eliminate dz/dt by invoking (3), (10) and (11) to get

$$R(r, z) = \frac{0.087 \sqrt{2/\nu\pi}\alpha\gamma^3}{\ln \Lambda} (1+z)N(r, z), \quad (18)$$

where (by Eq. 5) the number of particles inside r at redshift z can be expressed in terms of the final number of particles with which the halo is resolved $N_0 = M_0/m$:

$$N(r, z) = \frac{M}{M_0} N_0 e^{-\alpha z}. \quad (19)$$

The mass ratio entering into this last relation can be calculated *via* either Eq. (1) or Eq. (2).

The dimensionless relaxation time R has to be significantly greater than unity, at all z , if the simulated halo can be considered free of artificial relaxation inside radius r .³ What is required therefore is that

$$N_0 > 11.5 \frac{\sqrt{\nu/2}}{\pi\alpha\gamma^3} \ln \Lambda \frac{M_0}{M} \frac{e^{\alpha z}}{1+z}. \quad (20)$$

In Fig. 2 we show the variation of the of the quantity $(\frac{\gamma^3}{\ln \Lambda})N_0$ as a function of radius at different redshifts. The radii are expressed in terms of the final virial radius (at $z = 0$), by transforming them using Eq. (4). The cutoffs in the curves correspond to the virial radius at the denoted redshift (that is the maximum size of the halo considered at that redshift).

From this figure it is apparent that, provided $\gamma^3 \sim \ln \Lambda$,

³ Note that, because the virial radius and concentration are time dependent, accreted mass is not deposited uniformly; there is a preference, especially at later times, for mass increase in the outer regions (e.g., Zhao et al. 2003). However this implies that the characteristic time for mass change in the inner regions, where most of the relaxation occurs, is larger than that predicted by Eq. (6). The condition $R > 1$ thus constitutes a minimal requirement.

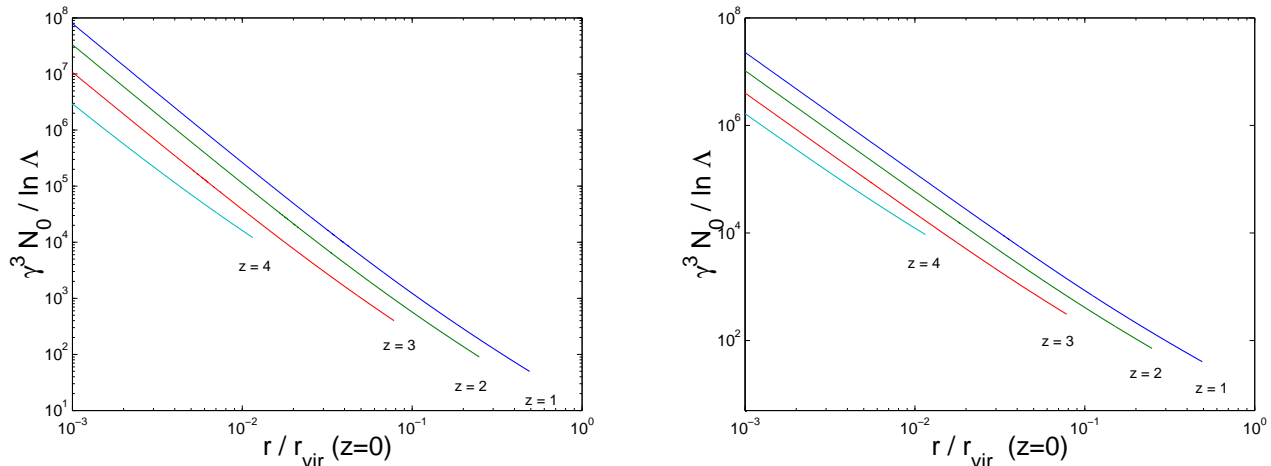


Figure 2. Number of particles N_0 required to compose a final main halo at $z = 0$ so that, at indicated redshifts, the mean relaxation time will be larger than the characteristic time for the halo to increase its mass at that redshift (see Eq. 6). Radii are rescaled to units of the virial radius at $z = 0$. The plot on the left corresponds to NFW haloes while that on the right to the M99 profile. Note that $\gamma^3 / \ln \Lambda \sim 1$

that artificial relaxation may have a dominant effect inside the inner $\sim 1\%$ of the final virial radius for $N_0 \sim 10^6$. Note that the demand for larger particle number is most stringent at larger times (smaller z). This is because the characteristic growth time τ_s is a steeply increasing function of z . The figure also suggests that, for fixed γ , the relaxation effects are more pronounced in the inner regions of NFW haloes, compared to the M99 case. Nevertheless, as we will see in Section 4.2, the introduction of variation in γ reverses this situation, since γ is significantly larger in the inner regions of NFW systems (this follows from the variations of the ratio of velocity dispersion to circular speed shown in Fig. B1).

3.2 Characteristic relaxation time for substructure

We consider a subhalo accreted at redshift z_a and remaining a separate dynamical system up to $z = 0$ — i.e., it stops growing, its outer regions are in fact stripped, but it keeps a dynamically distinct core. For this purpose we exploit the possibility of relating the relaxation and the local Hubble time; and in order to get simple closed form estimates, we will neglect relaxation at times $t < t(z_a)$ and focus on relaxation effects since accretion. From equations (15), (10) and (11) we can define a characteristic relaxation time

$$t_{\text{relax}}(r, z_a) = \frac{0.087\pi\gamma^3\sqrt{2/\nu}}{\ln \Lambda} \frac{M}{m} H^{-1}(z_a), \quad (21)$$

where M , ν , γ and Λ are all measured inside radius r at $z = z_a$. This timescale should be compared to the time interval separating the accretion epoch $t(z_a)$ and the end of the simulation at $t_0 = t(0)$. This determines a characteristic substructure relaxation time given by

$$t_{\text{rsub}}(r, z_a) = \frac{t_{\text{relax}}(r, z_a)}{t_0 - t(z_a)}. \quad (22)$$

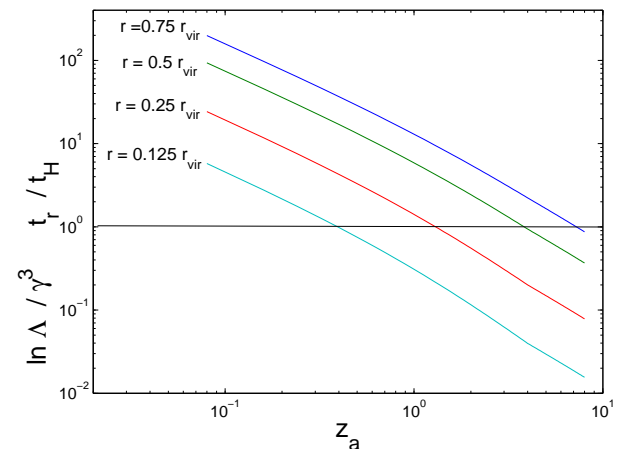


Figure 3. Relaxation time of substructure haloes consisting of a thousand particles accreted at redshift z_a . The timescales are expressed in terms of the time t_H elapsed between epochs z_a and $z = 0$ and are given at different fractions of the final virial radius. Values smaller than unity correspond to situations where the dynamics is completely dominated by artificial relaxation. Haloes are assumed to be of the NFW type

Now further assume that $t(z) = \frac{2}{3}H$ and $z = (t_0/t(z))^{2/3} - 1$, as is appropriate for an Einstein de-Sitter universe (in the next section we verify our results by undertaking the full calculation, including pre-accretion evolution, in the currently favoured “concordance” cosmology⁴). In this case we have

⁴ Note that while $t = t(z)$ for Λ CDM is quite different from that in an Einstein-de-sitter model the ratios $t(z_1)/t(z_2)$, entering into

$$t_{rsub}(r, z_a) = \frac{3}{2} \frac{0.087\pi\gamma^3\sqrt{2/\nu}}{\ln \Lambda} \frac{N(r, z_a)}{(z_a + 1)^{3/2} - 1}. \quad (23)$$

If, within some given radius, this quantity is less than unity the implication is that, by $z = 0$, the dynamics has become dominated by artificial discreteness noise.

In Fig. 3 we reproduce several plots where this dimensionless relaxation time, thus defined, is shown for haloes assumed to have $N(r_{\text{vir}}, z_a) = 1000$ when they are subsumed into their parent structures at different z_a (in the case of satellites haloes we only reproduce the results for NFW haloes, those for the M99 haloes are very similar). As can be seen, especially at relatively small radii, the relaxation time can be significantly smaller than the subhalo lifetime. Furthermore, it is to be noted that it will be this inner core of the subhalo that will survive stripping (see also Fig. 6 for more detail concerning the radial distribution of the relaxation time and Section 5.2 for a discussion of some possible consequences).

4 DIRECT CALCULATIONS

4.1 General considerations

From equations (12) and (13), the expected relative mean square perturbation due to discreteness imposed on to a test particle moving within an evolving cosmological halo is

$$\langle v_p^2/\sigma^2 \rangle = \frac{1}{2K} \sqrt{\frac{3G}{\pi}} \int_{t_f}^{t_0} \ln \Lambda(r, t) \frac{\sqrt{\nu(r, t)}}{\gamma^3(r, t)} \frac{\sqrt{\rho_c(t)}}{N(r, t)} dt. \quad (24)$$

The integral is evaluated within a given fixed fraction of the *final* virial radius $r_{\text{vir}}(t_0)$ — with the consequence that the radial coordinate contains an implicit time dependence (i.e. $r = r(t)$). The relations in Section 2.1 can be used to determine this dependence, as well as that of the other quantities entering into (24), provided the evolution of redshift as a function of time is known. For a flat universe with cosmological constant, the required transformations are given in Appendix A (in the calculations below we use $\Omega_V = 0.7$ and $h = 0.7$). Since the virial radius increases with time, a given fraction of the virial radius at $t = t_0$ will correspond to the whole virial radius at some earlier time. This naturally determines the lower limit of integration, the formation time t_f — for some fixed fraction of $r_{\text{vir}}(z = 0)$, it corresponds to a redshift z_f where this fraction is equal to whole virial radius $r_{\text{vir}}(z_f)$.

4.2 Relaxation of the most massive progenitors

In Fig. 4 we show the RMS perturbation due to particle noise, as a function of radius, expected for a halo with mass evolving according to Eq. 5 (with $\alpha = 1$) for several final values of the final total particle number N_0 . They are obtained by solving (24) using an adaptive integrator (NAG D01AJF) with a tolerance of 10^{-4} .

the equation below, differ by a factor of at most by $\sim 3\%$ for $10 \gtrsim z \gtrsim 1$ and by $\sim 30\%$ up to $z = 0$.

An interesting characteristic of the plots in Fig. 4 is the perfect power law behaviour of $\langle v_p^2/\sigma^2 \rangle^{1/2}$ over most of the radial interval. This is a consequence of a curious property of cosmological haloes, already noted by Taylor & Navarro 2001; namely the power law form of the phase space density. It is this phase space density, $\sim \rho/\sigma^3$, that determines the rate of relaxation. This property enables one to deduce a particularly simple fit for the variation of the relative RMS perturbation:

$$\langle v_p^2/\sigma^2 \rangle^{1/2} \approx 10^{-3} \sqrt{\frac{10^8}{N_0}} \frac{r_{\text{vir}}}{r}, \quad (25)$$

where r/r_{vir} refers to the fraction of the virial radius at $z = 0$. The number of relaxation times inside radius r can be counted as follows:

$$n(t_{\text{relax}}) = \langle v_p^2/\sigma^2 \rangle \approx 10^{-6} \frac{10^8}{N_0} \left(\frac{r_{\text{vir}}}{r} \right)^2, \quad (26)$$

which of course needs to be much smaller than one if artificial relaxation is to be negligible within radius r .

For $N_0 \lesssim 10^6$ then, particle motion is expected to be entirely dominated by noise in the inner percent of the virial radius; regions bounded by radii an order of magnitude smaller still having undergone ~ 100 relaxation times. These results are in agreement with the simple estimates presented in Section 3.1 (with the difference that the effect on M99 haloes are larger here, because variations in γ is taken into account).

The inner 0.1% is one relaxation time old even for $N_0 = 10^8$. Indeed, a final particle number inside the halo's virial radius of $N_0 = 10^{12}$ is required for noise to be reduced to the level of a few percent there. For a million particles this noise level is only reached at almost a third of the final virial radius; and this is larger than the average halo scale length $r_s = r_{\text{vir}}/c$ (c.f. Eq. 7).

Fig. 5 shows, for the inner percent of the final virial radius, the z -evolution of the relaxation rate (the integrand in 24) along with the principal components determining it. It shows that the relaxation rate decreases with redshift, for both the NFW and M99 profiles — the effect being more pronounced in the former case because the ratio of velocity dispersion to circular velocities that determines γ decreases faster with radius (Appendix B); and at smaller z because, for a given fixed fraction of the final virial radius, smaller radii are probed (recall that at z_f the whole virial radius corresponds to the inner one percent at $z = 0$).

Finally, note that, since new particles are continuously being introduced into the region, the way in which particles are affected by relaxation will differ, with the probable consequence that relaxation driven evolution can be expected to be different than in a static NFW type system.

4.3 Relaxation of subhaloes

In Fig. 6 we show the RMS perturbation in velocities expected as a result of particle noise for a subhalo composed of a thousand particles when it stops growing (after being incorporated into a larger structure). Before this, we assume that its mass grows at the exponential rate described by Eq. (5) with (as always) $\alpha = 1$. These results are in close

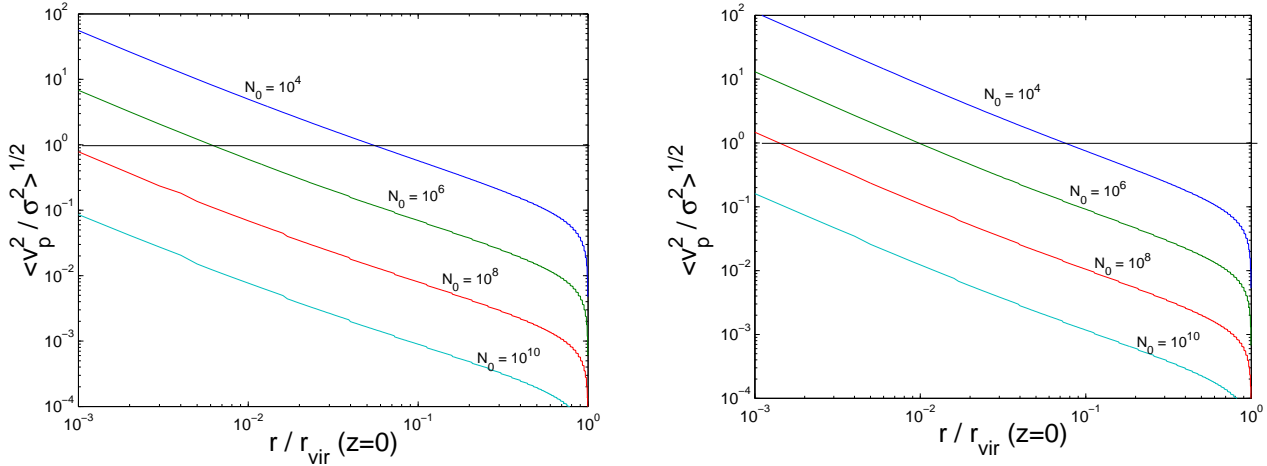


Figure 4. Expected RMS perturbation to the velocity resulting from particle noise in evolving most massive progenitor cosmological haloes. It is evaluated at a given fraction of the final virial radius by integrating Eq. (24), from the time when that fraction was equal to the whole virial radius at epoch $t = t_f$ up to $z = 0$ ($t = t_0$). Results for NFW haloes are shown on the left while those corresponding M99 ones are on the right

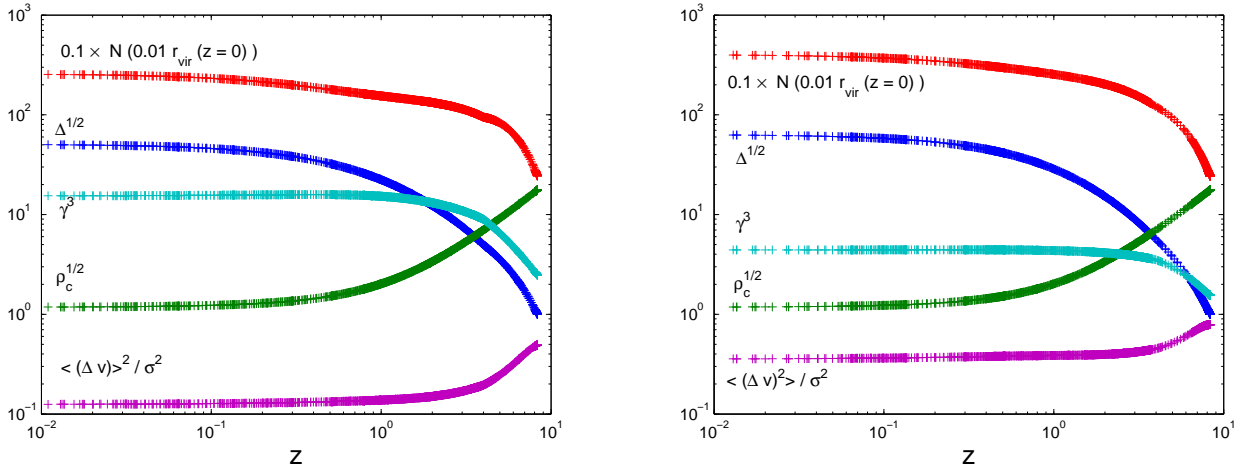


Figure 5. Instantaneous values of the perturbation to the velocities that arises from discreteness noise inside 1% of the final virial radius, and the corresponding magnitude of terms figuring in Eq. (eq:msdirect) that contribute to this quantity for NFW haloes (left) and M99 profiles. All contributions are of similar magnitude for the two profiles, except for the ratio of velocity dispersion to circular velocity, which is larger at small radii (hence lower redshift) in the NFW case. This leads to a somewhat smaller perturbation

agreement with the simple estimates derived in Section 3.2; they reinforce the conclusion that relaxation can be a significant factor determining the structure of subhaloes in simulations, their distribution and their effect on the parent halo structure (Section 5.2).

5 CONCLUSION

This paper presented an attempt at assessing the importance of particle noise in the evolution of collapsed cold dark matter structures, by generalising the diffusion formulation first proposed by Chandrasekhar to the case when the mass

distribution and radial extent of the system under consideration are variable. Although a most massive progenitor of a $z = 0$ halo will typically have increased its collapse mass by more than an order of magnitude by accreting subhaloes, at any given instant $\gtrsim 80\%$ of its mass is in a smooth component, most material in subhaloes having been stripped (e.g., Gao et al. 2004). This enables one to divide the analysis in two parts. In this context, ‘parent’ haloes, i.e. ones characterised by continuously increasing (virial) mass and radius throughout their evolution, were grown according to the empirical formula discovered by Wechsler et al. (2002). Subhaloes were treated differently, by assuming that their growth is arrested at accretion. Stripping was not explicitly

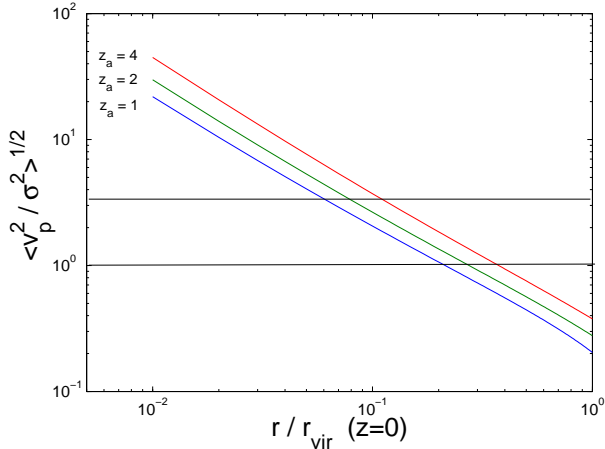


Figure 6. RMS perturbations to the velocity of satellite haloes composed of a thousand particles when they stop growing due to incorporation into a larger structure at the redshifts shown (up to which they are assumed to grow in mass, and hence particle number, according to Eq. 5). Results are obtained using Eq. (24) and correspond to subhaloes with NFW profiles. Horizontal lines show perturbations corresponding to (from bottom up) one and ten relaxation times

taken into account. But since it is in the inner region of subhaloes that relaxation is most significant, this does not appear to represent a major idealisation — as high resolution simulations, specially designed for the purpose of examining the issue, show the inner regions of stripped haloes to be largely unaffected (Kazantzidis et al. 2004).

We have derived simple closed form formulas for the characteristic relaxation times (Section 3), and also integrated the relevant equation characterising the expected RMS perturbation to the velocity directly (Section 4). The predictions of the two approaches agree quite closely. In what follows we summarise our results and sketch some possible consequences.

5.1 Relaxation in parent haloes

Our results were not found to be significantly affected by the exact form chosen for the evolution of the concentration parameter c or the parameter α characterising the mass growth rate (cf. Eq. 5), both quantities that are dependent on the final halo mass (in physical units), so this latter quantity does not enter directly into our presentation here, which is concerned only with the relaxation of particles *after* they have been accreted onto the most massive progenitor and are subsequently part of its smooth component (in the next two subsection we consider relaxation inside substructure, and briefly comment on the expected mass dependence of noise-induced relaxation in terms of merger history).

The power law (with index ~ -2) radial variation of the phase space density of cosmological haloes ensures a steep dependence of the relaxation rate, a linear function of this quantity, on radius. The perturbation due to discreteness

noise is adequately quantified by the empirical fits given in Section 4.2.

A test particle that is present inside the inner percent of the final virial radius, from the point in time when the virial radius of the halo was equal to this fraction, will experience a relative RMS perturbation to its velocity ~ 1 when the final halo is resolved with 10^6 particles — implying that its dynamics is completely corrupted by discreteness noise. In the very inner few thousandth of the final radius the RMS perturbation due to discreteness noise is an order of magnitude larger, meaning that these regions are of the order of a hundred relaxation times old.

In an evolving cosmological halo, particles are continually added within any given radius; it is also likely that some can gain energy (e.g. by interaction with sinking satellites; cf. El-Zant et al. 2004, El-Zant 2005) and move into trajectories with larger average radii. Particles that are accreted at a later stage are more mildly affected by relaxation. At any given fraction of the final radius therefore, there will be a range in the severity of artificial relaxation, depending on the accretion epoch of individual particles. This somewhat complex situation implies that effects of relaxation may be rather different than the familiar situation of fixed-mass systems, and therefore difficult to detect.

Our calculations thus represent a quantification of the magnitude of the perturbation of the discreteness noise, rather than its effect on the detailed dynamics and macroscopic structure. While it is quite probable that the significant role for artificial relaxation predicted by our analysis is reflected in the contradictory claims concerning the convergence and shape of the inner density profile of CDM haloes (Navarro et al. 2004; Diemand et al. 2005), with the predicted effect for static systems being a weakening of the cusp, further work is needed to determine the consequence in the case of evolving cosmological haloes.

The RMS perturbation to the velocities decreases as $\sim 1/\sqrt{N}$, implying that a parent halo needs to be resolved with $N \gtrsim 10^{10}$ particles at $z = 0$ if discreteness noise is not to dominate the dynamics of the inner 0.1% of the virial radius; and if it is to be negligible ($\langle v_p^2 / \sigma^2 \rangle^{1/2} \lesssim 1\%$) in the whole region where $r \gtrsim 0.1r_s \sim 0.01r_{\text{vir}}$. While perturbations of order unity are likely required for significant energy relaxation and restructuring of the azimuthally averaged density profile, much smaller perturbations may affect particle trajectories, with accompanying modification (isotropisation) of the velocity distribution and loss of triaxiality in spatially asymmetric systems (e.g., Merritt & Valluri 1996; see also Section 2.2).⁵

⁵ The reason this happens is due to a transition from regular to chaotic motion, which is very sensitive to perturbation. A very simple example of this phenomenon is the case of a pendulum on a ‘separatrix’ trajectory passing near the unstable (upper) equilibrium. Small perturbations can turn (regular) trajectories rotating in one direction into ones rotating into the opposite direction, or oscillating without a definite sense of rotation, or even transit between all these different possibilities (chaotic trajectories).

5.2 The relaxation of substructure

The results presented in this paper suggest that the situation with substructure is still more severe. A parent halo that is identified with $N_0 \sim 10^7$ has (from Eq. 5) $\sim 10^6$ particles at $z \sim 2$. Suppose a subhalo with $N_{\text{sub}} = 0.001N$ is then accreted. Assume that between redshifts two and one this 1000-particle halo will be stripped of $\sim 90\%$ of its mass (as would be expected from Gao et al. 2004 Fig. 14). For an NFW halo this also corresponds to a truncation of about 90% in radius. But according to Fig. 3, this inner region will be significantly affected by relaxation. In fact, by $z = 0$, it is expected to have undergone enough relaxation times to have approached core collapse! But this fate is only likely if it is not, in the meantime, dissolved by stripping.⁶

What effect is the significant relaxation expected to have on stripping? Cosmological haloes have a ‘temperature inversion’ in their inner velocity distribution (cf. Appendix B). Relaxation therefore causes initial expansion of the inner region, forming an isothermal core, before it re-contracts like a relaxing globular cluster (e.g., Hayashi et al. 2003). In the first phase, the core becomes less dense and more easily stripped; in the second the situation is reversed. Stripping is most efficient for subhaloes that venture near the centre of the parent, experiencing strong tidal forces. If, while the outer regions of a subhalo are stripped during successive passages, the inner region relaxes to a more diffuse density distribution, further stripping will be accelerated and the core may completely dissolve. Conversely, if the stripping is slow, there may be sufficient time for core contraction to take place. Further stripping is subdued and core dissolution becomes less likely.

If, as is suggested in several studies (e.g., Syer & White 1998; Dekel et al. 2003b; Dekel et al. 2003a), the structure of the halo profiles found in numerical simulations is dependent on the interaction between the subhaloes and their parents, then it is clear that such significant re-engineering of the subhaloes can be of major importance in determining the parent halo profile. It obviously also has implications for the number and spatial and orbital distribution of substructure. Given the discussion above, one would expect artificial relaxation to enhance the number of haloes that do not venture into the inner regions (i.e., those accreted on less eccentric orbits) and decrease the number of those that do venture there.

5.3 The N-scaling of the substructure-dominated relaxation time

The expectation from the results just outlined is that, beyond the inner percent or so of the final virial radius, relaxation will be dominated by particles inside substructure, or

⁶ Note that, because relaxation is quite a sensitive function of radius ($t_{\text{relax}} \sim r^2$ from Fig. 6 and Eq. 26) this same argument can be made for more central regions of more massive subhaloes (e.g., for the inner 1% of a subhalo consisting of 10% the mass of mass of the parent halo, accreted at $z \sim 2$ when the parent halo had $N \sim 10^6$), or more extended regions of less massive ones.

which have spent considerable time inside subhaloes before being stripped.

Simulations suggest that substructure has a mass function such that $dn/dm \sim m^{-9/5}$, quite independently of redshift (e.g., Gao et al 2004). If one ignores the logarithmic dependence, the relaxation time when expressed in units of dynamical time is, for any given subhalo, a linear function of the number of particles in it. Consider then a mean relaxation time averaged over subhaloes and normalised over an averaged dynamical time,

$$\langle t_{ra} \rangle \sim \frac{N_0 \int_{m_{\min}}^{m_{\max}} m \times m^{-9/5} dm}{\int_{m_{\min}}^{m_{\max}} m^{-9/5} dm}, \quad (27)$$

where the integration limits correspond to the least and most massive subhalo present. When the latter is orders of magnitudes more massive than the former, the above relation gives $\langle t_{ra} \rangle \sim N_0 m_{\max} m_{\min}^{4/5}$. If both m_{\min} and m_{\max} are independent of N_0 then the relaxation time scales linearly in with N_0 as in the standard case.

If, on the other hand, one supposes that, because of increasing resolution, $m_{\min} \sim 1/N_0$ (proportionately smaller haloes appear in the resolved field as N_0 increases) then $\langle t_{ra} \rangle \sim N_0^{1/5}$, which is roughly the scaling claimed by Diemand et al. (2004) on the basis of direct calculations of the relaxation time in the context of cosmological simulations. Their results also show that the N-scaling is closer to the canonical linear relation as one moves towards the centre of the main halo. This is also to be expected; since, near the centre, stripping causes the fraction of mass in subhaloes to decrease, while the relaxation in the smooth (parent halo) component becomes more efficient; and this scales roughly linearly with particle number.

Finally, note that although we have not followed the detailed merger history, the expectation derived from the work presented here is that relaxation is more enhanced in cluster haloes — since these form relatively recently, from particles that spend most of their existence inside poorly resolved structures. In contrast, a galaxy sized halo acquires most of its mass (i.e., particles) at larger redshift. It follows that, given the same resolution at $z = 0$, cluster halo particles would have, on average, been more affected by discreteness noise. This is in line with the conclusion reached by Diemand et al. (2004).

ACKNOWLEDGMENTS

I am indebted to Miloš Milosavljević for many valuable discussions and suggestions, as well as critical comments on an earlier version of this paper that led to significant improvement.

REFERENCES

- Athanassoula E., Vozikis Ch. L. Lambert, J. C., 2001, *A & A* 376, 1135
 Binney J., Tremaine S. 1987, *Galactic Dynamics*. Princeton University Press

- Bullock et al, 2001, MNRAS 321, 559
 Chandrasekhar S., 1943, Rev. Mod. Phys. 15, 1
 Dekel A., Arad I., Devor J., Birnboim Y., 2003, ApJ 588, 680
 Dekel A., Devor J., Hertzoni G., 2003, MNRAS 341, 326
 Diemand J., Moore B., Stadel J., Kazantzidis S., 2004, MNRAS 348, 977
 Diemand J., Zemp M., Moore B. Stadel J, Carollo M., 2005 (astro-ph/0504215)
 El-Zant A. A., 2002, MNRAS 331, 23
 El-Zant A. A., 2005 (astro-ph/0502472)
 El-Zant A. A., Shlosman I., 2002, ApJ 577, 626
 El-Zant A. A., Shlosman I., Begelman M. C., Frank J., 2003, ApJ 590, 641
 El-Zant A. A., Hoffman Y., Primack J. P., Combes F., Shlosman I., 2004, ApJ 607, L75
 Gao L, White S. D. M., Jenkins A., Stoehr F., Springel V., 2004, MNRAS 355, 819
 Huang S., Dubinski J, Carlberg, R. G., 1993, ApJ 404, 73
 Hayashi E., Navarro J. F., Taylor J. E., Stadel J., Quinn T., 2003, ApJ 584, 541
 Kazantzidis S., Mayer L., Mastropietro C., Diemand J., Stadel J., Moore B., 2004, ApJ 608, 663
 Kolb E. W., Turner M., 1990, The Early Universe. Addison Wesley
 Merritt D., Vallurri M., 1996, ApJ 471, 82
 Moore B., Quinn T., Governato F., Stadel T., Lake G., 1999, MNRAS 310, 1147 (M99)
 Navarro J. F., Frenk, C. S., 1997, ApJ 490, 493
 Navarro J. F. et al., 2004, MNRAS 293, 337
 Spitzer L., Hart M. H., 1971, ApJ 164, 399
 Syer D., White S. D. M., 1998, MNRAS 293, 337
 Tasitsiomi A., Kravtsov A. V, Gottlobler S., Klypin A. V., 2004, ApJ 607, 125
 Taylor J. E., Navarro J. F., 2001, ApJ 563, 483
 Wechsler R., Bullock J., Primack J., Kravtsov A., Dekel A., 2002, ApJ 568, 52
 Zhao D. H., Mo H. J., Jing Y. P., Borner G., 2003, MNRAS 339, 12

APPENDIX A: TIME DEPENDENCE OF ρ_C AND Z IN FLAT UNIVERSES WITH COSMOLOGICAL CONSTANT

According to Kolb & Turner (P. 55), for a flat universe with cosmological constant one has

$$t = \frac{2}{3} H^{-1} \Omega_V^{-1/2} \ln \left[\frac{1 + \Omega_V^{1/2}}{(1 - \Omega_V)^{1/2}} \right], \quad (\text{A1})$$

which, using $\Omega_V = \frac{\Lambda c^2}{3H^2}$ and $C_V = \sqrt{3\Lambda}c$ gives

$$\Omega_V^{1/2} = \frac{e^{C_V t} - 1}{e^{C_V t} + 1} \quad (\text{A2})$$

or equivalently

$$\frac{C_V}{3} \frac{e^{C_V t} + 1}{e^{C_V t} - 1} dt = -\frac{dz}{1+z}, \quad (\text{A3})$$

which by integration (with A the associated constant) gives

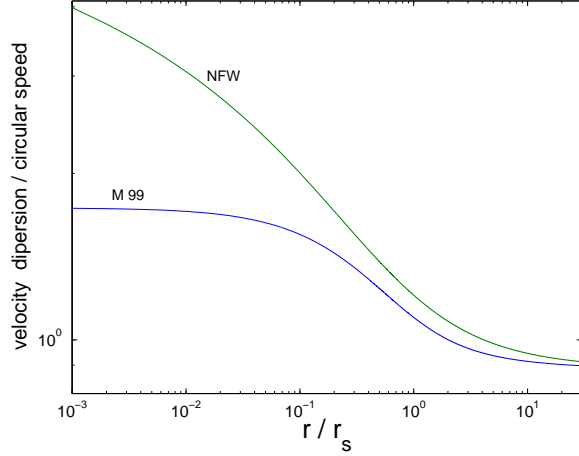


Figure B1. Velocity dispersion in spherical cosmological haloes with isotropic velocities in terms of the local circular velocities as a function of radius scaled to the halos scale length r_s .

$$1+z = \frac{e^{\frac{C_V}{3}t}}{A[e^{C_V t} - 1]^{2/3}}. \quad (\text{A4})$$

In a similar manner we find the critical density to vary as

$$\sqrt{\rho_C} = \frac{C_V}{2\sqrt{6\pi G}} \frac{e^{C_V t} + 1}{e^{C_V t} - 1}. \quad (\text{A5})$$

Using these formulas the integral in Eq. (24) can be evaluated with respect to the variable $C_V t$. When the constant in Eq. (A4) is evaluated by assuming $z = 0$ at $t = t_0$, the result does not depend on the value of t_0 . This is analogous to the familiar case whereas two body relaxation in an isolated system does not depend on the time elapsed in physical units, but instead on the number of dynamical times the system has been through.

APPENDIX B: VELOCITY DISPERSIONS

The Jeans equation for spherical system with isotropic velocity dispersion can be written as (e.g., Binney & Tremaine 1987)

$$\frac{d(\rho v_r^2)}{dr} = -\rho \frac{d\Phi}{dr}, \quad (\text{B1})$$

where $v_r^2 = \frac{1}{3}\sigma^2$ is the radial velocity dispersion. The general solution is

$$\rho v_r^2 = - \int \rho \frac{d\Phi}{dr} dr + C. \quad (\text{B2})$$

For any $\rho \rightarrow 0$, as $r \rightarrow \infty$, one must have $C = 0$, if the velocity dispersion is to be bound at large radii. The ratio of this unique physical solution to the local circular velocity is

$$\frac{v_r^2}{v_c^2} = \frac{\int_r^\infty \rho \frac{d\Phi}{dr} dr}{\rho \frac{d\Phi}{dr} r}, \quad (\text{B3})$$

the form reflecting the fact that, as opposed to circular motion, the velocity dispersion at any r is caused by particles that venture in and out of that radius.

For power law density distributions $\rho \propto r^{-n}$ solutions of Eq. (B2), with $C = 0$, imply that

$$\frac{\overline{v_r^2}}{v_c^2} = \frac{1}{2n - 2}, \quad (\text{B4})$$

for $n \neq 1$ and

$$\frac{\overline{v_r^2}}{v_c^2} = -\ln r, \quad (\text{B5})$$

($r < 1$). Note that, in the central regions, $\overline{v_r^2} \propto -r \ln r$ for the NFW profile and $\propto r^{1/2}$ for the M99 profile. Spherical cosmological haloes thus, necessarily, have a ‘temperature inversion’, at least as long as the velocity dispersion can be considered isotropic.

In Fig. B1 we reproduce the ratio of the three dimensional velocity dispersion to circular velocity for both profiles dealt with in this paper. It determines the value of *gamma* (corresponding to the average of this quantity within any given radius) that enter into the equations calculating the effects of relaxation.